

PHOTOMETRIC DISTANCES TO SMALL DARK CLOUDS: CB 24

DAWN E. PETERSON AND DAN P. CLEMENS

Department of Astronomy, Boston University, 725 Commonwealth Avenue, Boston, MA 02215; dpeterso@protostar.bu.edu, clemens@protostar.bu.edu

Received 1998 February 2; revised 1998 April 9

ABSTRACT

A new method for determining distances to dark clouds and small Bok globules based on broadband optical photometry has been developed. The method exploits the fact that M dwarf stars do not redden into the colors of other main-sequence stars. Consequently, from analysis of color-color diagrams of $V-I$ versus $B-V$, spectral types and extinctions of faint M dwarf stars located in front of and behind the molecular clouds can be established. For sufficiently deep observations ($B \approx 20\text{--}24$ mag), distances to clouds closer than about 1 kpc can be bracketed to a higher degree of precision (10–40 pc) than previously possible. Photometric data for the Bok globule CB 24 are used in this paper to demonstrate this method, yielding a maximum distance of 360 pc.

Key words: dust, extinction — ISM: clouds — ISM: globules — ISM: individual (CB 24) — stars: distances — stars: formation

1. INTRODUCTION

Establishing distances to small dark clouds is difficult whenever primary indicators such as ionizing stars or reflection nebulae are absent. The traditional method of determining distances utilized star counts (Bok & Bok 1941) or Wolf diagrams (Wolf 1923), which plot the number of stars versus apparent magnitude. However, these methods for distance determinations depend on questionable extrapolations of luminosity functions in order to work for small clouds. Alternatively, distances to small dark clouds can be assigned through association with nearby, larger molecular clouds. This method hinges on association between the small and larger cloud as demonstrated by close proximity and identical radial velocities, as well as primary distance knowledge for the larger cloud established via spectrophotometry of ionizing stars or reflection nebulae (e.g., Launhardt & Henning 1994, 1997). An additional method of assigning distances to small dark clouds entails bracketing the cloud distance by using spectroscopic distances to stars close in front of and behind the cloud to infer the cloud distance (Hobbs, Blitz, & Magnani 1986). Absent nearby associated large molecular clouds or stellar spectroscopic data, most small cloud distances have remained unknown.

Consequently, a new method for determining distances to small dark clouds has been developed based on the application of broadband photometry. From analysis of the visible-wavelength colors of stars in fields containing small dark clouds, many M dwarf stars can be easily identified. M dwarf colors are such that they do not redden into the colors of other main-sequence stars, an unusual property they share with early-type stars. However, unlike the very rare early-type stars, M dwarf stars are the most common stars in the solar neighborhood. This property makes M dwarfs excellent secondary distance indicators.

The locus of M dwarf $B-V$ versus $V-I$ colors is such that reddening and spectral type both may be determined from photometry alone. Thus, unextincted M dwarfs, those that are generally located in front of a highly extinguished region or dark cloud, and M dwarfs located behind a cloud, extinguished by the dust in the dark cloud, can both be found. Then, the farthest unextincted M dwarf toward the small dark cloud establishes the minimum cloud distance. Similarly, the nearest M dwarf extinguished by the small cloud dust

establishes the maximum cloud distance. For sufficiently deep images, enough faint M dwarf stars can be found to allow bracketing small cloud distances to 10–25 pc.

Distances to small dark clouds are needed in order to establish several important physical properties of these regions. First, they are necessary for obtaining luminosities of any embedded young stellar objects or protostars (e.g., Yun & Clemens 1990). In addition, they are necessary for calculating the masses and densities of the clouds (Clemens, Yun, & Heyer 1991). While volume densities for cloud cores can be obtained via millimeter-wavelength spectral line studies (e.g., Kane, Clemens, & Myers 1994, hereafter KCM), the core mass determinations require distance knowledge. Accurate information about the properties of small dark clouds is required in order to test models of these star-forming regions.

Bok globules are prototypical small dark clouds (≈ 0.1 pc in diameter) of molecular hydrogen and dust that are often sites of low-mass star formation (Keene et al. 1983; Yun & Clemens 1990). They generally have simple structures and are therefore ideal laboratories for studying isolated star formation. Bok globules have been loosely categorized as large and small; the “large globules” have masses greater than about $100 M_{\odot}$ and were cataloged by Barnard (1927) and Lynds (1962). The “small globules” have masses around $10 M_{\odot}$ and were cataloged by Clemens & Barvainis (1988, hereafter CB) and extended to the Southern Hemisphere by Bourke, Hyland, & Robinson (1995).

In this paper, a new method for determining distances to small dark clouds like Bok globules based on broadband photometric data acquisition and analysis of apparent M dwarf star colors is demonstrated for the Bok globule CB 24. CB 24 is a small, mostly spherically shaped Bok globule that has no associated *IRAS* point source and was not cataloged before CB. It is located in the second Galactic quadrant at $l = 155^{\circ}76$, $b = 5^{\circ}9$ ($\alpha = 04^{\text{h}}54^{\text{m}}33^{\text{s}}$, $\delta = 52^{\circ}11'07''$ [B1950.0]). The CO $J = 1 \rightarrow 0$ velocity was found by CB to be $V_{\text{LSR}} = 4.6 \text{ km s}^{-1}$. In addition, no *IRAS* extended emission for CB 24 was reported by Clemens et al. (1991). It was found by KCM that CB 24 and other similar small Bok globules are considerably less dense than are the dark cloud cores studied by Myers & Benson (1983). KCM concluded that the low column densities may indicate that Bok

TABLE 1
SUMMARY OF CB 24 OBSERVATIONS

Filter	Mean Air Mass	Integration Time (minutes)	PSF (pixels)	FWHM (arcsec)
B_J	1.06	90	7.3	2.9
V_J	1.07	10	7.9	3.2
I_C	1.08	10	5.5	2.2

globules like CB 24 have not yet undergone significant core contraction and represent a bona fide sample of “starless” small dark clouds.

The following sections elaborate the technique and analysis required to use the new method of distance determination for small dark clouds. Observations and data analysis performed for CB 24 are discussed in § 2. In § 3, the identification of reddened M dwarfs through the use of color-color diagrams is discussed. The calculation of color excesses and distance moduli of the identified reddened M dwarfs is also discussed in § 3, as well as reddening laws useful in obtaining these calculations. In § 4, we discuss the idea behind bracketing distances to the small dark clouds through distance knowledge of M dwarfs in the field, this distance analysis as applied to CB 24, and the results obtained. In § 5, the possible contamination of subdwarfs is discussed; we also present a Monte Carlo error propagation analysis to determine the uncertainties in the distances to the M dwarfs and the relative contributions from various sources of uncertainty. In § 6, we summarize our method and findings.

2. OBSERVATIONS AND DATA ANALYSIS

Observations toward the field containing CB 24 were performed using the Mount Laguna 1.05 m telescope operated by San Diego State University during 1994 December 30–1995 January 4. Images of the cloud and surrounding stars were obtained using a Tektronix 2048 × 2048 CCD through two Johnson filters and one Cousins filter: V_J , B_J ,

and I_C , respectively. The resulting images have 13.7×13.7 fields of view and 0.4 pixels. Table 1 summarizes information about the observations.

Standards were chosen from the Landolt (1992) compilation to span the wide range of colors expected for reddened M dwarfs ($B - V$ to +3) and were observed frequently to calibrate the atmospheric extinctions and filter transformations. Multiple dome flats were obtained and averaged to form final flats for each filter. Dark current is very low for the chip used ($< 1 e^{-1} \text{ pixel}^{-1} \text{ hr}^{-1}$); hence, no dark current corrections were applied. The images of CB 24, the standard-star images, and the flat fields were each bias-corrected and cleaned of cosmic rays. The CB 24 images and standards were then flat-fielded with their respective flats and visually examined. Images showing evidence of imperfect telescope tracking (as trailed stars) were rejected. For the B band, there were many good 10 minute duration images of CB 24, which were combined into one 90 minute effective duration image. Only one image was used for each of the visual and infrared bands.

The standards were analyzed using the DAOPHOT package in IRAF to measure instrumental magnitudes. The PHOTCAL package was used to develop a list of the observed magnitudes and a list of the corresponding Landolt (1992) standard magnitudes to permit obtaining transformation equations. Several different transformation equations were tried in order to develop fitting coefficients and uncertainties. Some of the parameters in the transformation equations were held constant and others were varied, thereby allowing experimentation for the best fit. Table 2 lists the final, best-fitting set of coefficients (represented by the lowercase letters and numbers) that were used in the transformation equations (also included in Table 2).

For the flat-fielded CB 24 images, synthetic aperture photometry was performed on the field stars using APPHOT in IRAF. Each image of CB 24—the combined blue image, the visual, and the infrared—was processed separately. Aperture corrections were computed from curves of growth for isolated intermediate-brightness stars in each image. These corrections were then applied to the observed instrumental

TABLE 2
FILTER TRANSFORMATION AND ATMOSPHERIC EXTINCTION VALUES

Coefficient	Value (Uncertainty)
$m_V = V + v_1 + v_2 X_V + v_3(B - V) + v_4(B - V)X_V + v_5 X_V^2$	
v_1	3.430 (0.043)
v_2	0.301 (0.022)
v_3	0.039 (const)
v_4	-0.018 (const)
v_5	-0.040 (const)
$m_B = [(B - V) + V] + b_1 + b_2 X_B + b_3(B - V) + b_4(B - V)X_B$	
b_1	3.724 (0.023)
b_2	0.303 (0.012)
b_3	-0.061 (const)
b_4	-0.036 (const)
$m_I = [V - (V - I)] + i_1 + i_2 X_I + i_3(V - I) + i_4(V - I)X_I$	
i_1	4.233 (0.017)
i_2	0.035 (0.009)
i_3	-0.076 (const)
i_4	0.028 (0.002)

NOTES.— X_V is the air mass of the observation in filter V , X_B is the air mass of the observation in filter B , and X_I is the air mass of the observation in filter I .

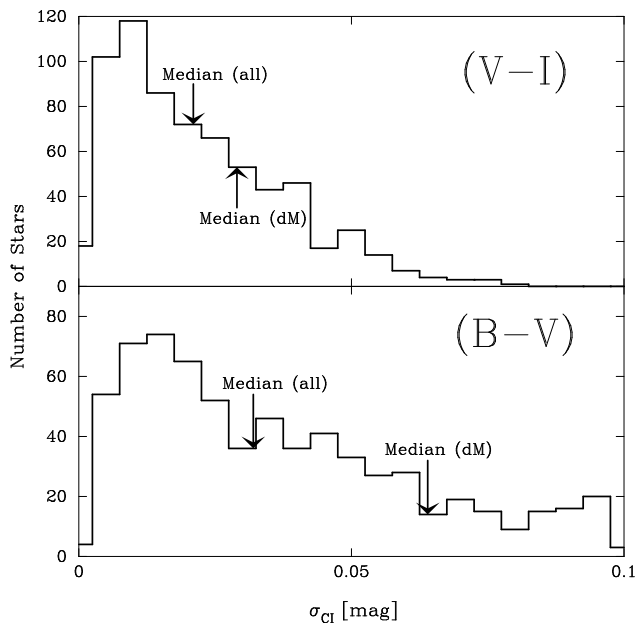


FIG. 1.—Uncertainty histograms of the $V-I$ and $B-V$ colors for all 678 CB 24 field stars.

magnitudes. The resulting list included the instrumental visual magnitudes of 831 stars in the CB 24 field that were positionally matched across all three filters. The standard-star filter-atmosphere transformation equations were inverted to convert instrumental magnitudes in the CB 24 frames to apparent V -band magnitudes and $B-V$ and $V-I$ color index (CI) values, as well as their uncertainties.

To ensure high-quality results in the analysis, a maximum color uncertainty of 0.1 mag was permitted, resulting in calibrated color indexes for 678 CB 24 field stars (matched in all three filters). Histograms of uncertainties of the $B-V$ and $V-I$ colors for the 678 CB 24 field stars are displayed in Figure 1. A comparison of median uncertainty values in $V-I$ for all 678 stars and for the 15 candidate M dwarf stars (see § 3) shows that they are consistent. For $V-I$, the value of the median uncertainty for all 678 stars is 0.021 mag, and the median uncertainty value for the 15 M dwarfs is 0.029. In contrast, for $B-V$, the value of the median uncertainty for all 678 stars is 0.032 mag while the median uncertainty value for the 15 candidate M dwarfs is 0.064 mag. The median uncertainty for the 15 candidate M dwarfs in $B-V$ is significantly higher than for all 678 stars, showing that our ability to find faint M dwarfs remains B -magnitude limited. The median B magnitude for the 15 candidate M dwarfs is 21.4 mag—a challenging value for small telescopes.

3. DISTANCE METHOD

The method for determining distances to small dark clouds employs four steps in the postobserving analysis. First, a $V-I$ versus $B-V$ color-color diagram is constructed for the field stars. For the 678 CB 24 field stars with $\sigma_{CI} < 0.1$ mag, the $V-I$ versus $B-V$ color-color diagram is displayed in Figure 2. Second, M dwarf stars are identified in the $V-I$ versus $B-V$ diagram. Third, color excesses $E(B-V)$ and absolute magnitudes are obtained for the M dwarf stars. Fourth, distances are established for the extinguished and unextinguished M dwarfs to bracket the small dark cloud distance.

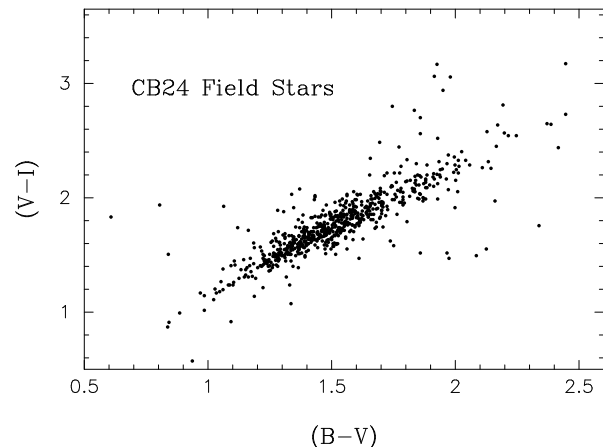


FIG. 2.— $V-I$ vs. $B-V$ color-color diagram of 678 stars in the CB 24 field whose color index uncertainties are less than 0.10 mag.

3.1. M Dwarf Colors

As can be seen in the color-color diagram of Figure 2, the CB 24 field stars are mostly clustered together along a diagonal locus, with a few scattered outlying stars. The diagonally clustered stars in the CB 24 field represent a blend of extinguished giants and main-sequence stars. Consequently, the only stars about which anything certain can be inferred are the outlying stars. In the $V-I$ versus $B-V$ color-color diagram, the information we seek will be obtained from stars that lie above the locus of diagonally clustered stars. The nature of the outlying stars that appear below the color-color diagram is not known. Coordinates for these stars (and all of the stars in the field) appear in Peterson (1998).

Unextinguished M dwarf stars will lie along a different locus in the $V-I$ versus $B-V$ color-color diagram than the giants and remaining main-sequence stars. In order to quantitatively obtain that M dwarf locus, $B-V$ and $V-I$ colors of known late K and M dwarfs were drawn from the literature (Leggett 1992; Weis 1993). In addition, colors of Hyades members were included (Eggen 1974; Johnson & Knuckles 1955; Johnson, Mitchell, & Iriarte 1962; Leggett, Harris, & Dahn 1994; Pels, Oort, & Pels-Kluyver 1975; Taylor & Jone 1985; Uppgren 1974; Uppgren & Weis 1977; Uppgren, Weis, & Hanson 1985; van Altena 1966, 1969; van Bueren 1952; Weis 1983; Weis, DeLuca, & Uppgren 1979; Weis & Uppgren 1982). To the Weis (1993) list of dwarf K and M stars, we applied an offset to the original published data of -0.025 in $B-V$ and of $+0.055$ in $V-I$ to match the Leggett and Hyades values. To obtain an average M dwarf locus in the color-color diagram, stars were $V-I$ binned (from values of 0.8 to 3.3) into bins 0.05 mag wide and were $B-V$ binned (from values of 0.5 to 1.9) in increments of 0.025 mag. The resulting histograms of number versus $B-V$ at constant $V-I$ showed peaked distributions and so were then each fitted with a Gaussian. The resulting $B-V$ means and uncertainties were assigned to their corresponding $V-I$ bins. The median value for the widths (FWHMs) of the Gaussian curves in all the bins, which represents the intrinsic spread of the M dwarf colors in the $B-V$ direction, was found to be 0.063 mag. Systematic effects due to metallicity are undoubtedly important and are only partially accounted for in our approach. Nevertheless, polynomials were fitted to the run of mean

TABLE 3
SUMMARY OF PROPERTIES OF CANDIDATE REDDENED M DWARFS TOWARD CB 24

ID (1)	X (pixels) (2)	Y (pixels) (3)	V (mag) (4)	B-V (mag) (5)	V-I (mag) (6)	A _V (mag) (7)	M _V (mag) (8)	Distance Modulus (mag) (9)
1.....	78.9	841.0	19.83 ± 0.035	1.66 ± 0.071	2.20 ± 0.036	0.56 ± 0.34	9.47	9.80 ± 0.40
2.....	1118.3	747.8	16.08 ± 0.004	1.66 ± 0.007	2.35 ± 0.004	0.51 ± 0.06	10.04	5.53 ± 0.36
3.....	264.3	588.2	19.71 ± 0.030	1.69 ± 0.064	2.48 ± 0.029	0.53 ± 0.33	10.47	8.71 ± 0.43
4.....	1305.7	1312.1	17.55 ± 0.006	1.77 ± 0.013	2.44 ± 0.007	0.83 ± 0.11	9.89	6.82 ± 0.35
5.....	1038.1	239.0	16.62 ± 0.006	1.74 ± 0.011	2.80 ± 0.008	0.68 ± 0.37	11.33	4.61 ± 0.41
6.....	1519.2	1840.9	19.58 ± 0.028	1.83 ± 0.055	2.77 ± 0.027	0.95 ± 0.36	10.81	7.82 ± 0.41
7.....	1818.8	1872.9	19.19 ± 0.018	1.86 ± 0.046	2.70 ± 0.019	1.05 ± 0.22	10.44	7.70 ± 0.38
8.....	1065.3	1274.9	18.92 ± 0.017	1.86 ± 0.036	2.56 ± 0.017	1.10 ± 0.19	9.90	7.92 ± 0.36
9.....	1079.2	1160.2	19.29 ± 0.023	1.93 ± 0.046	2.52 ± 0.022	1.44 ± 0.29	9.24	8.61 ± 0.36
10.....	269.9	360.9	19.73 ± 0.031	2.19 ± 0.074	2.81 ± 0.030	2.35 ± 0.45	8.89	8.48 ± 0.44
11.....	774.1	1053.8	19.86 ± 0.034	2.45 ± 0.091	3.17 ± 0.036	3.13 ± 0.54	8.95	7.78 ± 0.46
12.....	1444.7	479.0	20.11 ± 0.040	1.95 ± 0.089	2.94 ± 0.040	1.30 ± 0.51	10.87	7.94 ± 0.47
13.....	1953.9	427.0	20.13 ± 0.041	1.98 ± 0.090	3.06 ± 0.040	1.42 ± 0.52	11.11	7.61 ± 0.49
14.....	1313.8	1407.5	19.87 ± 0.035	1.92 ± 0.071	3.06 ± 0.034	1.20 ± 0.45	11.45	7.23 ± 0.46
15.....	1966.0	694.1	19.64 ± 0.033	1.93 ± 0.066	3.17 ± 0.033	0.98 ± 0.40	12.12	6.54 ± 0.46

$B-V$ versus $V-I$ to establish an ad hoc description of the unextincted M dwarf locus. The best-fitting fourth-order polynomial is

$$B-V = -1.40 + 3.35(V-I) - 1.12(V-I)^2 + 0.02(V-I)^3 + 0.032(V-I)^4. \quad (1)$$

The polynomial is a good description for $B-V$ from 1.4 to 1.9 and $V-I$ from 1.6 to 3.1. The M dwarf color values from the literature and the polynomial fit are displayed in Figure 3.

M dwarf stars located in the CB 24 field will lie along, near, or, if reddened, to the right of the mean M dwarf locus in the $V-I$ versus $B-V$ color-color diagram. As seen in Figure 2, though, there are no stars in the CB 24 field that lie directly along or within 0.1 mag of the locus. Thus, all of the M dwarfs in the CB 24 field have been reddened; we detect no unreddened M dwarfs. This prevents determining a minimum allowed distance for CB 24 from these data.

In order to identify the M dwarf stars in the field of CB 24, analysis of the color-color diagram resulting in separation of M dwarf stars from other main-sequence stars is required. Generally, M dwarfs are identified as being

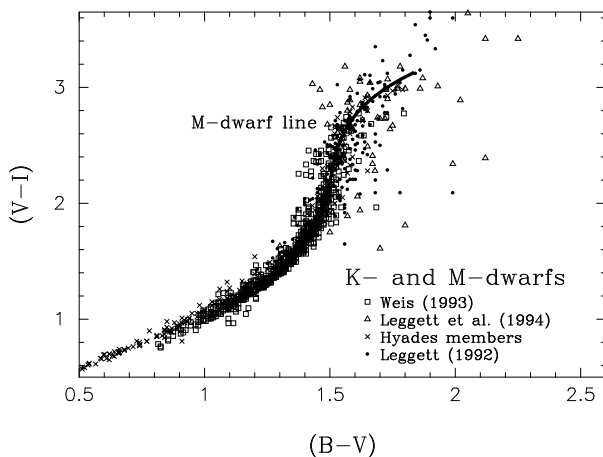


FIG. 3.— $V-I$ vs. $B-V$ color-color diagram of known K and M dwarf stars from the literature. The least-squares-fitted M dwarf line appears superposed on the plot.

located at redder $B-V$ and $V-I$ values in the color-color diagram than on the locus of unextincted M dwarfs. They must also show colors different from those of the other field stars.

For CB 24, a median-filtered linear least-squares fit was performed on the diagonal field star color-color distribution for stars with $B-V$ colors greater than 1.4 mag. The width σ of the field star locus in $V-I$ was measured in the fitting process to be 0.094 mag. Stars whose colors were found to be greater than 3σ away from the linear fit were identified as possible candidate M dwarfs. Twenty-nine stars were found to be located more than 3σ from the linear fit, but only 15 of those were located above the locus of field stars, in the region in which extincted M dwarfs lie. Consequently, we identify these 15 as candidate reddened M dwarf stars near CB 24, and they are indicated by the triangles in the color-color diagram of Figure 4.

Table 3 presents summary information about the 15 candidate reddened M dwarfs toward CB 24. Column (1) gives an identification number of the M dwarf. Columns (2) and (3) give the X- and Y-coordinates, respectively, of each M dwarf as it appears in the V -band image of Figure 5.

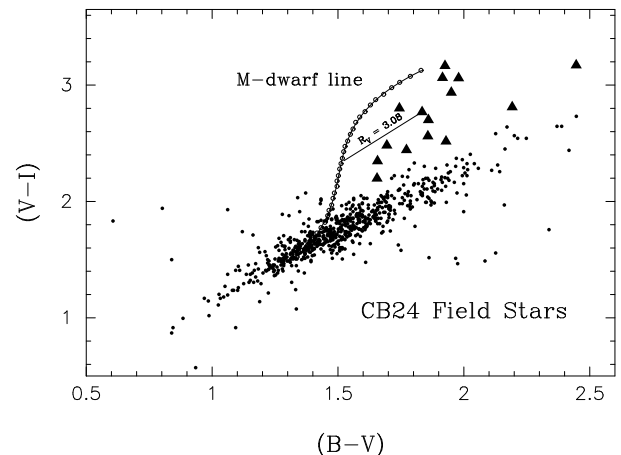


FIG. 4.— $V-I$ vs. $B-V$ color-color diagram of the CB 24 field stars. The average M dwarf line is superposed in open circles, and the triangles represent the 15 CB 24 field stars that are candidate reddened M dwarf stars. The reddening line indicated has a slope of 1.35, which corresponds to $R_V = 3.08$.

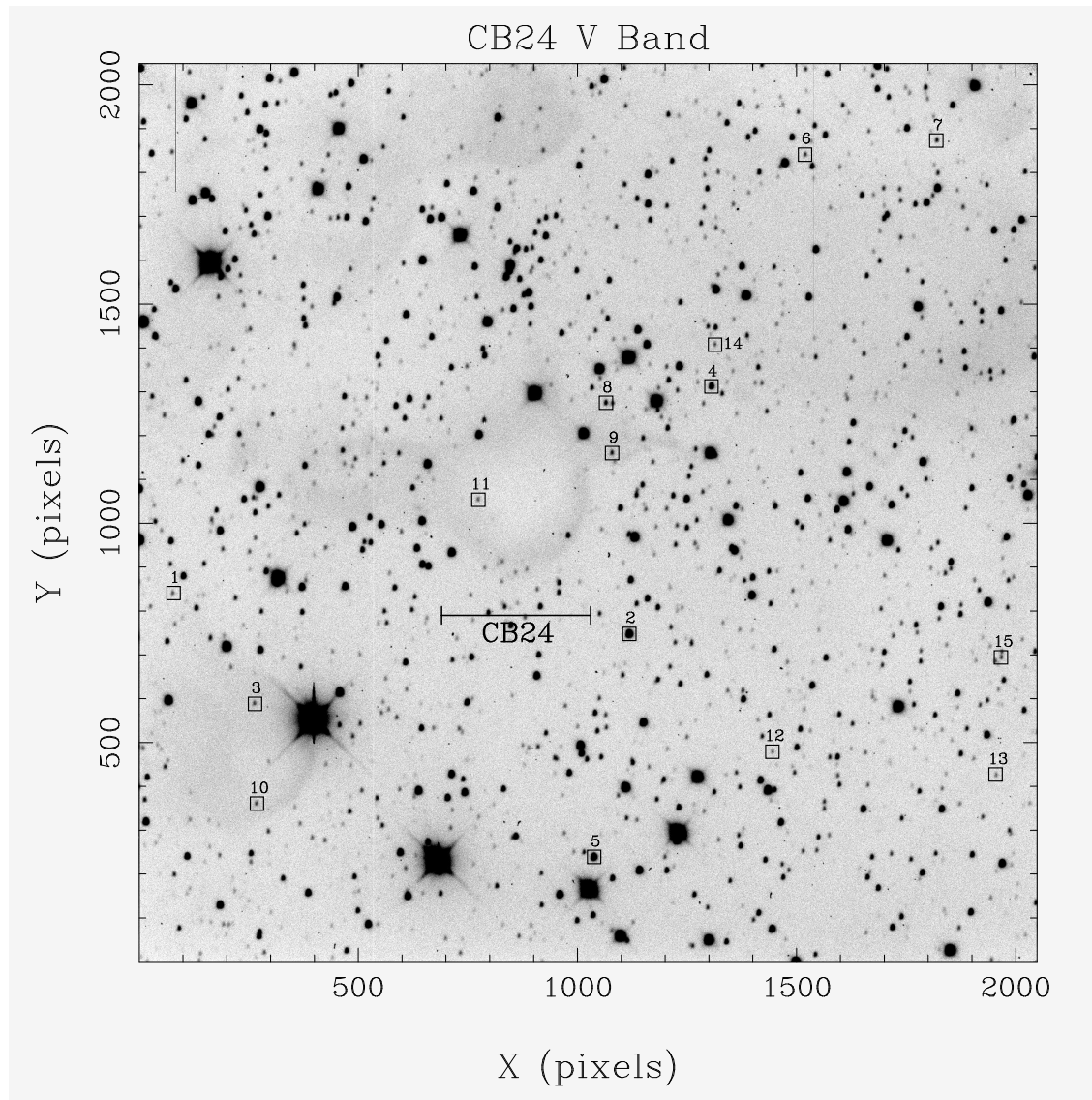


FIG. 5.—CB 24 V-band image. The 15 candidate reddened M dwarfs are boxed and numbered according to Table 3.

Columns (4), (5), and (6) indicate the V , $B-V$, and $V-I$ values, respectively, for each M dwarf along with their observed uncertainties.

3.2. Reddening Laws

Establishing distances to the reddened M dwarfs requires dereddening their colors. In the $V-I$ versus $B-V$ diagram, dereddening consists of sliding the point representing a reddened M dwarf parallel to a “reddening line” (see Fig. 4) until the point arrives on the unextinguished M dwarf locus at its intrinsic color values. However, the *slope* of the reddening line $E(V-I)/E(B-V)$ depends on the ratio of the total amount of extinction to the color excess:

$$R_V = A_V/E(B-V). \quad (2)$$

The ratio R_V depends on the mean dust grain size and may change with location in small dust clouds. Generally, R_V values are known to range from below 3 to at least 6.

The extinction law analyses of He et al. (1995) were used to investigate reddening law effects. The He et al. work was used instead of Rieke & Lebofsky (1985) because the former reported values for Cousins I (our I filter choice) while the latter adopted the Johnson I passband, and the differences

between the systems are profound. For the He et al. mean reddening curve, an average value for the color excess slope [i.e., the ratio $E(V-I_C)/E(B-V)$] is 1.35 and the mean ratio of total to selective extinction R_V is 3.08 ± 0.05 .

Analysis of the effects resulting from changes in the R_V factor requires additional knowledge of the ratio of extinction for the filters of interest, here A_{I_C}/A_V . Following He et al., the relationship between the color excess slope and the extinction ratio is

$$\frac{A_\lambda}{A_V} = \frac{E(\lambda - V)}{R_V E(B-V)} + 1, \quad (3)$$

where $\lambda = I_C$. Data provided in He et al. (1995) included values of $E(B-V)$, $E(V-I_C)$, and R_V for 154 highly obscured OB stars in the Milky Way. Using their A_{I_C}/A_V and R_V values between 2.5 and 4, we performed a least-squares fit to quantify the relationship:

$$\frac{A_{I_C}}{A_V} - 1 = -1.18 + 0.37R_V - 0.0422R_V^2. \quad (4)$$

Color excess slopes can be calculated by rearranging equation (3) to accommodate the least-squares fit solution

from equation (4), as

$$\frac{E(V-I_c)}{E(B-V)} = R_V \left(1 - \frac{A_{I_c}}{A_V} \right). \quad (5)$$

Within the appropriate range for R_V , this final equation relating R_V to the color excess slope is a cubic. Nevertheless, the rather wide range of R_V (2.5 and 4 are the limits in the He et al. distribution of R_V) corresponds to a rather narrow range of the color excess slope (between 1.3 and 1.5).

As will be described in § 5, we performed experiments using a range of R_V values to examine for the effects of different reddening laws on the cloud distances obtained. Once an appropriate R_V value and corresponding color excess slope have been chosen, the total $B-V$ color excess, $E(B-V) = (B-V) - (B-V)_0$, for each candidate reddened M dwarf can be estimated. The value of $(B-V)_0$ is found from the intercept of the M dwarf locus and the reddening line for the chosen color excess slope and measured color data for a particular star. Extinctions A_V can then be calculated using equation (2), the $E(B-V)$ values, and the R_V value corresponding to the chosen color excess slope. The extinction values for the 15 candidate reddened M dwarfs, calculated based on $R_V = 3.08$, are recorded in column (7) of Table 3. These extinctions were then used to correct the apparent visual magnitudes, m_V , for each of the M dwarfs.

The last step in the process of finding the distance moduli is calculating the absolute magnitudes, M_V , for each of the M dwarf stars and comparing these with the extinction-corrected apparent magnitudes. From a best-fit linear relationship found by Reid (1991) between absolute magnitude M_V and $(V-I)_0$ colors for M dwarf stars,

$$M_V = (2.89 \pm 0.20) + (3.37 \pm 0.07)(V-I)_0, \quad (6)$$

the absolute V magnitudes for the 15 M dwarf stars were calculated after performing the dereddening correction and are listed in column (8) of Table 3. Using the extinction-corrected m_V values, the distance moduli to the M dwarf stars were calculated, and these values are recorded in column (9) of Table 3. For all of the values listed in columns (8) and (9) in Table 3, an average value $R_V = 3.08$ (with corresponding color excess slope 1.35) was used.

4. RESULTS

In order to best find the distances to a small dark cloud using our distance method, it would be ideal to possess distances to M dwarfs located both in front of and behind the cloud, thereby bracketing the distances to the cloud. These M dwarfs may not always be present. In this case, inferences can be made about the distances to M dwarfs located near and to the side of the cloud instead of directly in front of or behind the cloud, although these estimates result in less accurate bracketed distances. Consequently, merely possessing the distance moduli to the M dwarf stars in the field surrounding CB 24 does not immediately result in a precise distance to CB 24.

Distances to extincted M dwarfs near CB 24 were found by the method previously discussed. As can be seen in the V -band image of the CB 24 field in Figure 5, with the 15 candidate reddened M dwarfs boxed, many of the M dwarfs appear to lie on or behind areas of high extinction. In Figure 6, we plot the derived extinctions A_V versus the calculated distance moduli for the 15 candidate reddened M dwarfs. But, as indicated above, the areas of high extinction are not all necessarily associated with the CB 24 cloud.

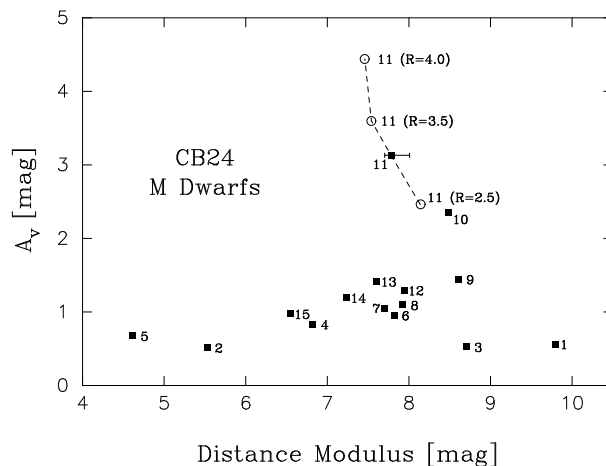


FIG. 6.—Extinction vs. distance modulus for the 15 reddened M dwarfs, labeled according to Table 3. The dashed line represents the locus for star 11 for various reddening laws, indexed by the R_V values shown. The error bars on star 11 correspond to the 50% range for reddening values given by He et al. (1995).

4.1. Maximum Distance: Star 11

Fortunately, one of the extincted M dwarf stars whose distance modulus has been obtained (star 11) is projected within the optical boundary of CB 24. The extremely red colors of star 11 are a strong argument that the star is highly extincted; hence, we conclude that star 11 is not located in front of the cloud. Kassebaum (1996) presents near-infrared K -band magnitudes for stars projected onto CB 24. Three stars in Table 3 (stars 8, 9, and 11) have analogs in his list. The K -band magnitude for one star (our star 4) was measured directly from the K -band image (T. Kassebaum 1996, private communication). Using our derived absolute magnitudes, extinctions, and distance moduli for these four stars, we predicted apparent K -band magnitudes for comparison.

In general, the agreement between our predicted K magnitudes and the measured values is good. However, when the magnitude difference is plotted versus A_V , a trend is present. The sense of the trend is that for $A_V \approx 0.8$ (star 4) the difference magnitude is zero and increases to 1.3 mag by star 11 ($A_V \approx 3$). Thus the K -band observations of star 11 show it to be about 1.3 mag brighter than we predicted.

This could partially be explained by the lack of a color term in the calibrations of Kassebaum (1996)—his observations were performed only in the K band, and MgCdTe imagers like the one he used have some K -magnitude shifts with stellar color. However, based on colors of M dwarfs and typical MgCdTe calibrations (Yun & Clemens 1995), we predict a brighter K mag by only about 0.05 mag for each 1 mag of $B-V$ reddening.

Alternatively, a lightly modified combination of absolute magnitude, extinction, reddening law variation, and distance modulus for star 11 could produce the observed K -band magnitude. However, a single modification to any one of these parameters cannot easily reproduce the K -band magnitude. We conclude that our optical band assessment of star 11 is consistent with that seen in the K band.

In addition, gas column densities toward CB 24 measured by Kane (1996) using ^{13}CO radio spectral line mapping are consistent with the extinction we measure for star 11. Thus we conclude that star 11 cannot be located in

front of the cloud. It may be located within the cloud, though *IRAS* observations show no evidence of dust heating. It is most likely that star 11 is on the back side of CB 24, furnishing a firm upper limit to the cloud distance.

Using the He et al. (1995) extinction law average value for R_V of 3.08 and the corresponding color excess slope of 1.35, the distance modulus for star 11 is calculated to be 7.78 mag, resulting in a maximum distance to CB 24 of 360 pc.

4.2. No Minimum Distance

Once the distance to a star located in front of the CB 24 cloud is obtained, a minimum distance to CB 24 will be established. Unfortunately, the images of CB 24 we obtained did not show such unextinguished stars. Obtaining deeper images, particularly in the *B* band, would not be expected to reveal many distant foreground M dwarf stars. Looking deeper in the *B* band could reveal unextinguished, intrinsically redder stars than we have seen. However, their faint intrinsic brightnesses would be virtually undetectable beyond a few tens of parsecs, limiting their ability to establish a useful minimum cloud distance.

5. DISCUSSION

5.1. Subdwarf Colors and Contamination Effects

One potential problem with the notion that the indicated CB 24 M dwarf candidates are indeed reddened M dwarfs is that their colors are similar to the colors of M and K subdwarfs and extreme subdwarfs. Spectral type and luminosity classifications of subdwarfs and extreme subdwarfs were made spectroscopically by Gizis (1997). Subdwarfs reside below (or to the left of) the main sequence in the (*V*, *B*−*V*) color-magnitude diagram because of their metal deficiency, being Population II stars with $[M/H] = -1.2 \pm 0.3$. Extreme subdwarfs are even more metal-poor, with $[M/H] = -2.0 \pm -0.5$. Metal-poor subdwarfs (another class of stars that falls between subdwarfs and extreme subdwarfs in metallicity) tend to have redder *B*−*V* colors at a given *V*−*I*. Consequently, metal-poor subdwarfs have colors very similar to our candidate reddened M dwarfs. Spectroscopy is required to definitively establish whether each of our candidates is an M dwarf or a subdwarf. However, spectroscopic observations of the CB 24 stars are not available, so another approach is necessary.

Using the luminosity function for cool dwarfs surveyed by Kirkpatrick et al. (1994), we estimated that it is unlikely for our candidate reddened M dwarf stars to be subdwarfs. Out of the 133 objects in the Kirkpatrick et al. sample, spectroscopic analysis determined that 124 were M dwarfs, seven were M giants, and two were marginal M subdwarfs. The contamination of M subdwarfs in the Kirkpatrick et al. sample of M dwarfs was less than 2%. Direct integration of the subdwarf luminosity function (e.g., Dahn et al. 1995), assuming observational completeness to *V* = 20 and for *V*−*I* colors redder than 1.6 mag, yields a prediction of much less than one subdwarf in the CB 24 field. Therefore, we expect that of the 15 candidates boxed in Figure 5, virtually all should be reddened M dwarfs.

5.2. Errors and Uncertainties

The uncertainty in the reddening slope and the degree to which it affects the distance modulus were explored directly in order to determine to what degree the distance to CB 24 depends on reddening. Referring again to Figure 6, different reddening slopes were used to compute values for the esti-

mated extinction to star 11 and the corresponding distance moduli. With $R_V = 2.5$ (the lower R_V limit seen by He et al.) and its corresponding color-color slope of 1.3, the resulting distance modulus for star 11 was found to be 8.14 mag. This calculated distance suggests a strong upper limit to the distance modulus because almost all observed values of R_V are greater than 3.0. For an $R_V = 4.0$, which corresponds to a slope of 1.5, the distance modulus was found to be 7.46 mag. Hence, one estimate for a reasonable range of the distance modulus for the M dwarf star located behind the CB 24 cloud is 7.46–8.14 mag (310–425 pc).

Although using different R_V values to identify a range of distances is an effective way of exploring reddening law effects, calculations of uncertainties in the distances must include additional sources of error. Uncertainties in the distances to the M dwarfs, and consequently to CB 24, include observational uncertainties, uncertainties in the location of the M dwarf locus and its intrinsic width in the color-color plane, reddening law effects, and uncertainties in the conversion from intrinsic colors to absolute magnitudes. We explore the effects of each of these in the following.

Because of the inherent nonlinearities in the distance method calculations, in order to include the effects of each of the above-mentioned uncertainties into a total uncertainty for the distance modulus and extinction, a Monte Carlo approach was adopted. The effect of each measured uncertainty was simulated by calculating a large number of random values drawn from Gaussian distributions characterized by the original means and their associated uncertainties or widths.

Each uncertainty effect was individually modeled and applied. First, each observational data value was replaced by random values from Gaussian distributions keyed to the observed *V*, *B*−*V*, and *V*−*I* values and uncertainties. Next, reddening law effects were modeled to match the He et al. (1995) data, for which we find a mean R_V of 3.06 and distribution width of 0.327. Then the conversion from intrinsic colors to absolute magnitudes was modeled using the values in equation (6) to create related families of synthetic conversion equations. Finally, to take into account the location and width of the M dwarf locus, the mean values and uncertainties calculated for the “average” M dwarf locus (discussed in § 3.1) were modeled to create fam-

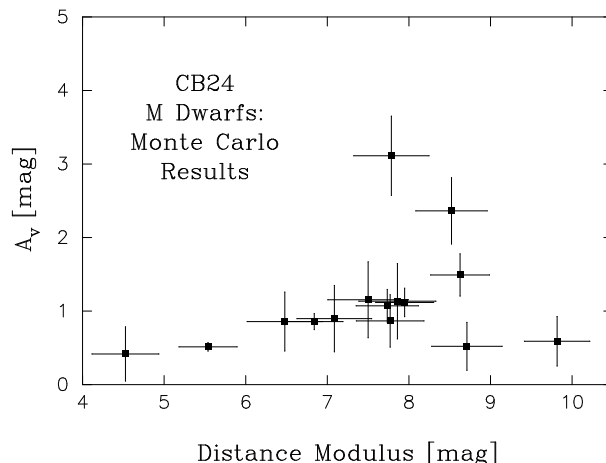


FIG. 7.—Extinction vs. distance modulus for the 15 reddened M dwarfs. The calculated mean A_V and distance modulus values and corresponding error bars were calculated from the distributions of synthetic values generated for each star using 1000 Monte Carlo iterations.

TABLE 4
ERROR BUDGET

Method Stage	Estimated Uncertainty in A_V (%)	Estimated Uncertainty in Distance Modulus (%)
Measured colors	40	15
Reddening slope	3	5
M dwarf line	15	5
Absolute magnitude	4	50
Slope	3	30
Offset	2	40

ilies of M dwarf loci. All of the new model values, representing the original values and uncertainties, were then propagated through the model functions to produce synthetic values of A_V and distance modulus for 1000 simulations of each of the 15 candidate M dwarfs. Mean values and dispersions of the resulting Monte Carlo concentrations of synthetic A_V and distance moduli values were calculated and are represented in Figure 7 by error bars. The Monte Carlo derived uncertainties are also listed in Table 3 in columns (7) and (9).

To estimate the effective contribution of each individual uncertainty effect to the total uncertainty, each effect was successively “turned off” by setting its corresponding Gaussian model width to zero in order to ascertain the percentage change in the total uncertainty. Table 4 presents the reduction effect on the total error produced by eliminating each component. Observational uncertainties generate the largest effect on A_V values, while errors in the conversion of intrinsic colors to absolute magnitudes have the largest effect on the distance moduli estimates. Changes in the reddening law do not appear to have much effect on either A_V or distance modulus, as modeled with the Monte Carlo method. This is a stronger statement than the simple limits established from consideration of the points plotted in Figure 6.

Therefore, to improve this distance method, it would be advantageous to obtain a better absolute magnitude conversion (eq. [6]) as well as more precise observational measurements in order to develop more accurate estimates of extinctions and distance moduli. Because the absolute magnitude conversion step produced such a large contribution to the total error budget, we examined it further by individually zeroing the errors in the slope and offset terms of equation (6). As shown at the bottom of Table 4, these contribute roughly equally to the total error, and hence both need to be improved. However, it should be noted that

much of the absolute magnitude conversion uncertainty is due to the intrinsic spread of real stellar values (Dahn et al. 1995).

6. SUMMARY

A method for determining distances to small dark clouds like Bok globules using photometric techniques has been described and demonstrated using observations of a field containing the Bok globule CB 24. These observations were obtained in the B , V , and I filters, allowing a $V-I$ versus $B-V$ color-color diagram to be developed. Analysis performed on this color-color diagram resulted in the identification of 15 reddened M dwarf stars. Using known colors of M dwarf stars, as well as known extinction laws and reddening factors, color excesses and distance moduli for the reddened M dwarf stars were established. From these distance moduli, the maximum distance to the cloud was determined to be 360 pc.

Even though CB 24 has a fairly small optical extent, a maximum distance to the cloud was established, largely because of the fortuitous location of star 11. Most other small dark clouds are larger than CB 24, and this method will be useful for finding their distances.

This research was supported by NSF grant AST 92-21194 and NASA grants NAG 5-1997 and NAG 5-3337. The Mount Laguna Observatory is operated by San Diego State University (SDSU), and these observations were conducted as part of their external guest observer program. We would like to thank Bob Leach for providing the CCD instrumentation and software. Brian Kane assisted in the SDSU observations. We thank Lida He for clarifications regarding the reddening law data. Tom Kassebaum provided a copy of his M.S. thesis, a K -band FITS image of the CB 24 field, and many hours of productive discussion. Comments from Ken Janes and an anonymous referee led to substantial improvements.

REFERENCES

- Barnard, E. E. 1927, *A Photographic Atlas of Selected Regions of the Milky Way. II. Charts and Tables* (Washington: Carnegie Inst. Washington)
- Bok, B. J., & Bok, P. F. 1941, *The Milky Way* (Cambridge: Harvard Univ. Press)
- Bourke, T. L., Hyland, A. R., & Robinson, G. 1995, *MNRAS*, 276, 1052
- Clemens, D. P., & Barvainis, R. 1988, *ApJS*, 68, 257 (CB)
- Clemens, D. P., Yun, J. L., & Heyer, M. H. 1991, *ApJS*, 75, 877
- Dahn, C. C., Liebert, J., Harris, H. C., & Guetter, H. H. 1995, in *The Bottom of the Main Sequence—and Beyond*, ed. C. G. Tinney (Berlin: Springer), 239
- Eggen, O. J. 1974, *PASP*, 86, 697
- Gizis, J. E. 1997, *AJ*, 113, 806
- He, L., Whittet, D. C. B., Kilkenny, D., & Spencer Jones, J. H. 1995, *ApJS*, 101, 335
- Hobbs, L. M., Blitz, L., & Magnani, L. 1986, *ApJ*, 306, L109
- Johnson, H. L., & Knuckles, C. F. 1955, *ApJ*, 122, 209
- Johnson, H. L., Mitchell, R. I., & Iriarte, B. 1962, *ApJ*, 136, 75
- Kane, B. D. 1996, Ph.D. thesis, Boston Univ.
- Kane, B. D., Clemens, D. P., & Myers, P. C. 1994, *ApJ*, 433, L49 (KCM)
- Kassebaum, T. 1996, M.S. thesis, San Diego State Univ.
- Keene, J., Davidson, J. A., Harper, D. A., Hildebrand, R. H., Jaffe, D. T., Loewenstein, R. F., Low, F. J., & Pernic, R. 1983, *ApJ*, 274, L43
- Kirkpatrick, J. D., McGraw, J. T., Hess, T. R., Liebert, J., & McCarthy, D. W., Jr. 1994, *ApJS*, 94, 749
- Landolt, A. U. 1992, *AJ*, 104, 340
- Launhardt, R., & Henning, T. 1994, in *ASP Conf. Ser. 65, Clouds, Cores, and Low Mass Stars*, ed. D. P. Clemens & R. Barvainis (Provo: ASP Press), 224
- . 1997, *A&A*, 326, 329

- Leggett, S. K. 1992, ApJS, 82, 351
Leggett, S. K., Harris, H. C., & Dahn, C. C. 1994, AJ, 108, 944
Lynds, B. T. 1962, ApJS, 7, 1
Myers, P. C., & Benson, P. J. 1983, ApJ, 266, 309
Pels, G., Oort, J. H., & Pels-Kluyver, H. A. 1975, A&A, 43, 423
Peterson, D. E. 1998, B.A. Distinction thesis, Boston Univ.
Reid, I. N. 1991, AJ, 102, 1428
Rieke, G. H., & Lebofsky, M. J. 1985, ApJ, 288, 618
Taylor, B. J., & Joner, M. D. 1985, AJ, 90, 479
Uppgren, A. R. 1974, ApJ, 193, 359
Uppgren, A. R., & Weis, E. W. 1977, AJ, 82, 978
Uppgren, A. R., Weis, E. W., & Hanson, R. B. 1985, AJ, 90, 2039
van Altena, W. F. 1966, AJ, 71, 482
———. 1969, AJ, 74, 2
van Bueren, H. G. 1952, Bull. Astron. Inst. Netherlands, 11, 385
Weis, E. W. 1983, PASP, 95, 29
———. 1993, AJ, 105, 1962
Weis, E. W., DeLuca, E. E., & Uppgren, A. R. 1979, PASP, 91, 766
Weis, E. W., & Uppgren, A. R. 1982, PASP, 94, 475
Wolf, M. 1923, Astron. Nachr., 219, 109
Yun, J. L., & Clemens, D. P. 1990, ApJ, 365, L73
———. 1995, AJ, 109, 742